FORECASTING TECHNIQUES

A Neural Network Short-Term Forecast of Significant Thunderstorms

DONALD W. MCCANN

National Severe Storms Forecast Center, Kansas City, Missouri

(Manuscript received 3 February 1992, in final form 6 April 1992)

ABSTRACT

Case studies are the typical means by which meteorologists pass on their knowledge of how to solve a particular weather-forecasting problem to other forecasters. A case study helps others recognize an important pattern and enhances the meteorologist in the meteorologist–machine mix. A neural network is an artificial-intelligence tool that excels in pattern recognition. This tool can become another means of enhancing a forecaster's pattern-recognition ability. Since neural networks are a relatively new tool to meteorologists, some basics are given before discussing a 3–7-h significant thunderstorm forecast developed with this technique. Two neural networks learned to forecast significant thunderstorms from fields of surface-based lifted index and surface moisture convergence. These networks are sensitive to the patterns that skilled forecasters recognize as occurring prior to strong thunderstorms. The two neural networks are combined operationally at the National Severe Storms Forecast Center into a single hourly product that enhances pattern-recognition skills. Examples of neural network products are shown, and their potential impact on significant thunderstorm forecasting is demonstrated.

1. Introduction

The operational weather forecaster in the meteorologist–machine mix is evolving from a raw-data analyzer to an interpreter of the machine output. Machines handle numerical computations very well, while the human brain can interpret data and recognize patterns better than a machine. Enhancing the strengths of each results in improved weather forecasts. Each new generation of computers has allowed better modeling of the atmosphere, and much of the emphasis on improved forecasts has been placed on the machine.

Enhancing the meteorologist means improving his/her pattern-recognition ability. Much of the research in pattern recognition is in presenting case studies. These case studies arise when one meteorologist recognizes a pattern and shares it with another. However, the patterns associated with a particular weather phenomenon are not always easy to see. Artificial-intelligence (AI) techniques are being developed to enhance meteorologists' pattern-recognition proficiency. Moninger (1990) provides a good summary of current AI research in thunderstorm forecasting.

Two successful AI techniques are expert systems and neural networks. Expert systems are just what the name implies. A knowledge engineer tries to extract the knowledge from one or more experts who know how to solve the problem in question. Many times the knowledge engineer and expert are the same person. Decision trees, which are popular in many weather offices, are simple expert systems. Bullas et al. (1990) and Weaver and Phillips (1990) are examples of current expert-system forecast tools.

Neural networks, on the other hand, do not require any prior knowledge of a solution. A neural network "learns" what it needs to know about a particular problem. It is very similar to a grade schooler learning the alphabet. Once a student learns the letter "A," the letter can take on various looks (lower case, cursive, etc.) yet still be the letter "A." Neural networks have solved many problems in pattern recognition. Some examples are speech recognition, speech synthesis, vision and image processing, robotics and autonomous vehicles, game playing, financial forecasting, and gambling analysis (Stanley 1988). Frankel et al. (1990) are developing a neural network to forecast lightning strikes.

The National Aviation Weather Advisory Unit (NAWAU) of the National Severe Storms Forecast Center (NSSFC) has a responsibility to issue hourly advisories (called WSTs) for significant thunderstorm complexes to aviation users throughout the continental United States. Significant to aviation are thunderstorms that are in long lines or large clusters, are embedded, or are capable of producing tornadoes or large hail. WST issuances always imply severe or extreme turbulence, severe icing, and low-level wind-shear potential. In addition, unit forecasters also issue a 2–6-h outlook each hour outlining areas where they expect to issue future WSTs.

Corresponding author address: Donald W. McCann, U.S. Department of Commerce, NOAA/NSSFC, 601 East 12th Street, Room 1728, Kansas City, MO 64106.

They use many tools in developing these outlook areas, but primary among them are computed fields of surface-based lifted index and surface moisture convergence. Some patterns of these two fields are known to be precursory to significant thunderstorms (Ostby 1975, 1984; Darkow and Livingston 1975; Hales and Doswell 1982; Maddox and Doswell 1982; Hirt 1982; Doswell 1982; Livingston and Wilson 1986; Bothwell 1988; Waldstreicher 1989). For years, the author, as one of the WST forecasters, has overlaid these two fields to make thunderstorm forecasts, and indeed many favorable patterns have preceded significant thunderstorm development by several hours. Improving the recognition of these favorable patterns suggests a neural network experiment.

There has been little research done with neural networks in meteorology, yet they have the potential to solve pattern-recognition problems that other methods have not yet been able to solve. This paper will introduce neural networks in general before discussing the neural networks developed for a significant thunderstorm outlook. Then the potential impact of the neural-network forecasts on operational meteorology will be discussed.

2. What are neural networks?

Humans are terrible number crunchers when compared with a computer. On the other hand, humans excel in pattern recognition. A young baby can easily recognize its mother's face. Using traditional techniques, a computer must be extensively programmed to recognize even simple facial patterns. Although humans are good at pattern recognition, they still have many problems in recognizing patterns because of subtleties in what they perceive or because of the shear complexity of the problem.

That is where artificial intelligence becomes a helpful tool. The goals of any AI technique are twofold. The first is to help learn potential solutions to problems so that humans can recognize them better. The second is to help bring less knowledgeable people up to skill levels of those with greater knowledge.

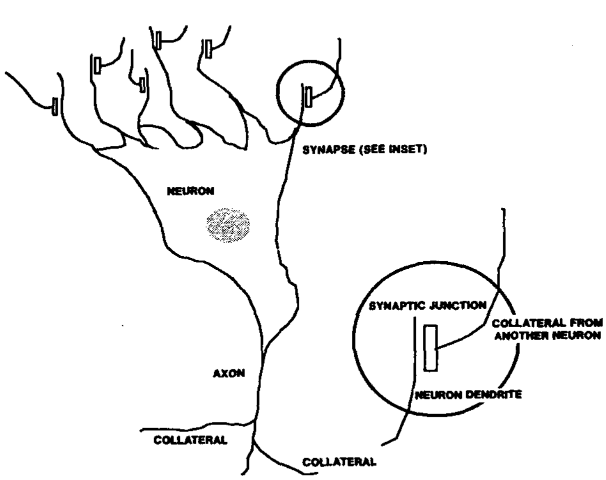

FIG. 1. Diagram of a typical brain nerve cell (taken from Caudill 1990).

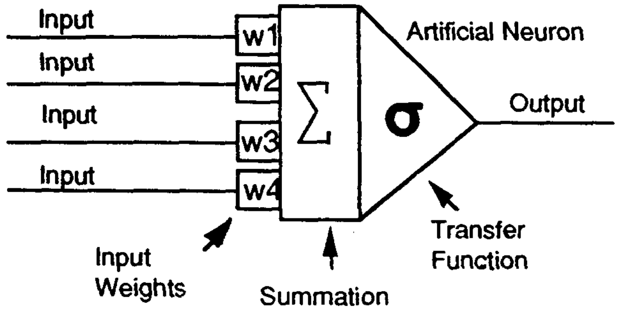

FIG. 2. Diagram of an artificial neuron. Input is multiplied by the weights, then all the products are summed. This sum becomes the argument of the transfer function. The result of the function is the neuron's output. (Taken from Stanley 1988).

Neural networks are constructed much like that of a human brain. In the brain there are 100 billion nerve cells (neurons), each connected to perhaps thousands of other cells (Fig. 1). A stimulus of some kind (example: listening to a piano) starts the process of a series of neurons firing from the ear to the brain. The first neuron receives the input then decides whether or not to fire. If it does not fire, the signal ends there. But if it does fire, it sends the signal down its axon to other neurons. Each connection at the synaptic junction has chemicals that enhance or inhibit the signal. The next neuron then sums the input from the previous neuron and all others to which it is connected. Then it decides to fire or not depending on this sum. The process continues until the brain recognizes the stimulus. Deciding a response is part of this process. After receiving the same stimulus often, the brain will respond in a predictable way. This is called learning.

An artificial neuron works in the same way (illustrated in Fig. 2). Each input is multiplied by the weight of its connection with the neuron. The connection weights may be positive (stimulative) or negative (inhibitive). The connection weights help determine which inputs are important and which are not. All the inputs are summed. Then a transfer function determines the output. The output from one neuron may be connected to many others and becomes those others' input.

There are many kinds of neural networks. Back-propagation networks are easy to implement and have solved many kinds of problems and are therefore the most popular (Caudill 1990). A simple back-propagation network is shown in Fig. 3. It has one input layer of neurons and one output layer and often has one or more hidden layers between the input and output layers. Each of the neurons in a layer is connected to each of the neurons in the layer below. The network learns by example. A teacher shows the network a set

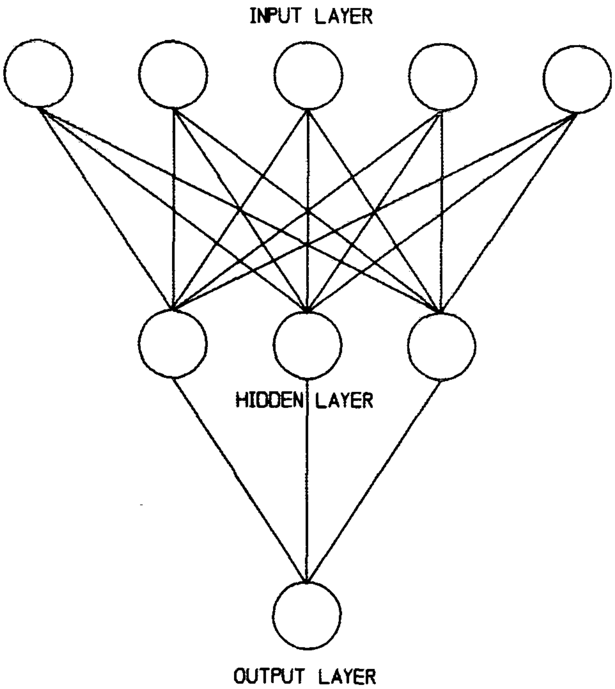

FIG. 3. Schematic diagram of a back-propagation neural network showing the connections of each of the neurons.

of inputs that flow through the connection weights into the hidden layer, which, in turn, produce output to the output layer via their own connection weights. The output layer contains the network's response to the input. The teacher then compares this output with the desired output. If the error between the two is small enough, the network has learned that input. If not, the error is back-propagated through the network by adjusting the connection weights. Then the input is presented again, and again, if necessary, until the network output is close to the desired output. *It is the connection weights between the input and output layers through the hidden layer that store the knowledge of the neural network.*

The teacher shows the network as many patterns and variations to those patterns that the problem suggests. When the network has learned most or all of them, the network is considered trained. The teacher then presents a set of inputs the network has not seen and tests its ability to recognize the correct patterns. If testing is successful, then the network can be used to predict output from any input data.

The approach to input and output is similar to screening regression (Charba 1979) and multivariate (McNulty 1981) methods of statistics, and back-propagation is a fitting technique similar to these statistical methods. However, a neural network is highly nonlinear so it can resolve many problems traditional statistical methods cannot. Furthermore, a neural network needs fewer examples to learn than statistical approaches, as long as the examples represent the entire spectrum of expected patterns.

3. Training the neural networks

Thunderstorms do not form just anywhere. Thunderstorms need a favorable environment in which to develop. This favorable environment, in its most elemental analysis, requires just two ingredients to come together. One is a potentially unstable air mass, and the other is a lifting mechanism to start the release of the instability. There are no magic amounts of each component that ensures thunderstorm development (Bothwell 1988). In fact, a low quantity of one may be compensated by an abundance of the other (McCann 1988). Operational meteorologists frequently observe this. That is the challenge of thunderstorm forecasting.

There are many ways to measure potential instability and to infer upward motion from surface synoptic observations. Edman (1989) describes a surface-based lifted index (LI) that is popular with NSSFC forecasters because it is calculated hourly from surface data and forecast 500-mb temperatures. When the boundary layer is well mixed, it provides an excellent representation of the instability of the atmosphere (Hales and Doswell 1982). Deducing upward motion from horizontal processes is a complicated task because it involves analyzing the atmosphere at all levels. Surface moisture flux convergence provides a good measurement of low-level processes that provide initial lift for thunderstorms (Waldstreicher 1989).

Surface-based LI and moisture divergence values are calculated hourly on NSSFC's Centralized Storm Information System (CSIS) on a 1° grid spacing for the continental United States and adjacent areas (Hirt 1982; Edman 1989). Note the moisture advection term is not calculated on CSIS. As explained later, this is not a critical omission. A 7×7 subgrid was centered on randomly chosen points on 1800 UTC data collected from 132 days from April to August 1990 over the eastern two-thirds of the United States (Fig. 4). On most days, two points (or cases) were selected from each of the four subregions in order to get a representative range of possible conditions. Other size subgrids were possible, but the 7×7 subgrid appeared to be large enough to depict the relevant patterns and small enough so computations would not bog down. So, for each case, the input to the neural networks was 49 points of LI and 49 points of moisture divergence, or 98 total neurons. Network input has to be between zero and one in the back-propagation network algorithm used for this experiment. Therefore, the LI inputs were linearly normalized over the range from +5 to −12. Values higher than +5 were treated as +5 and values lower than −12 were treated as −12. Moisture divergence values were similarly normalized over a range from +30 to -60×10^{-1} g kg^{-1} h^{-1}.

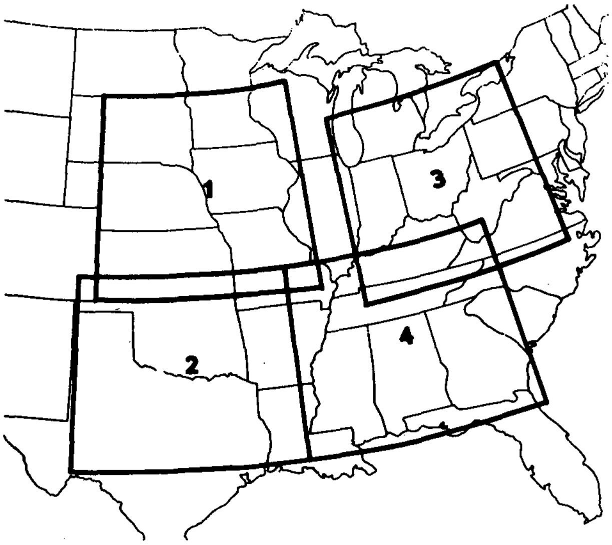

FIG. 4. Map showing where the random points were chosen in this study. On most days, two points from each region were chosen.

One set of tested networks (NN0) normalized the highest LI and moisture divergence values to zero and the lowest to one. Another set of networks (NN1) was tested with the opposite normalization. Looking at this normalization method from a different perspective, NN0 networks are learning how to forecast areas of significant thunderstorms. On the other hand, NN1 networks are learning how to forecast areas of no significant convection; the remainder outlines areas of significant thunderstorms. The network output to learn was a WST issued (1) or no WST issued (0) for the 3–7-h period after 1800 UTC, the desired outlook period.[1] Neural networks can resolve "fuzzy" data, so if a WST was issued at an adjacent grid point but not at the point itself, the output was a "maybe" (0.5). Initially there were approximately 600 points in the learning set, but since the "no WST issued" cases were highly duplicative and overwhelmed the rest of the data, about three-quarters of these null cases were randomly eliminated to speed the learning process. The teaching dataset consisted of 275 points.

Two parameters can be varied easily to produce an optimum network solution: the size of the hidden layer and the structure of the transfer function. The hidden layer lies between the input and output layers. Recall that the weights that connect the hidden layer with the input and output layers hold the neural network's "knowledge" of the problem. If a hidden layer is too small, it will not be able to learn what it needs to know. Conversely, if a hidden layer is too large, it will only learn the inputs presented to it and has trouble generalizing (Stanley 1988). Single hidden layers of 30, 50, and 80 neurons were tried for this project. Stanley (1988) suggests that a hidden layer be one-half the size of the sum of the input (98) and output (1) layers, and indeed the 50 neuron hidden-layer networks produced the fastest learning and the best test results in both kinds of networks. (Testing is explained below.)

The transfer function is a sigmoid function of the form

$$f(x) = 1/(1 + e^{-wx}).$$

Figure 5 shows that a sigmoid function varies from zero to one. The steepness of the function near zero varies with the weight parameter, w. High values of w predominately transfer values out of the neuron closer to zero and one; low values of w provide a more even distribution. The weight parameter was varied after the best hidden-layer size was found to determine the best neural network for each type of normalization. A w of 3 was best for the neural network that specifically forecast thunderstorms (NN0), while a w of 2 was best for the "no thunderstorm" network (NN1).

Training the networks was difficult because of the complexity of the input. The accepted practice in teaching a neural network is to let it run until it has learned all of the input cases (Caudill 1991). However, no network learned more than 175 cases in any one scan of the data, even after 4000 passes. (The program ran on a 20-MHz 80386 PC machine for over 48 hours.) This was a vexing problem. Initially it was thought that the neural-network technique was not going to be successful. Nevertheless, when tested on 150 independent datasets randomly withheld from the original 750 points, the best neural network of each type got more than 85% of the outputs correct, indi-

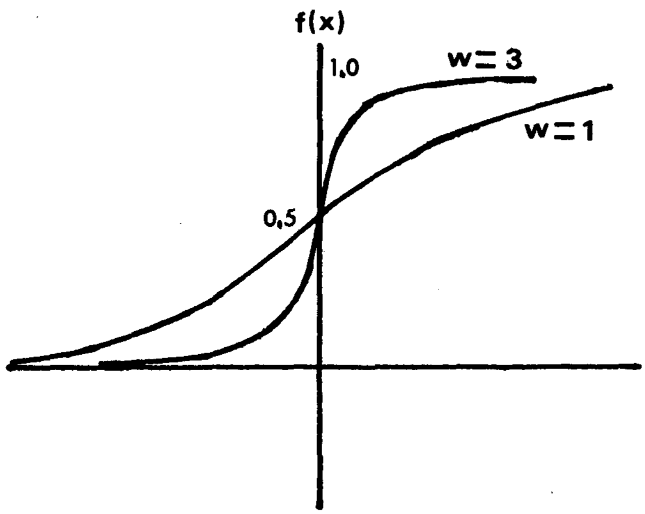

FIG. 5. Diagram of two sigmoid functions. See text for the function definition.

[1] WSTs are issued by NAWAU forecasters at 55 min past each hour—for example, 1855 UTC. The 2–6-h outlook is really 3–7 h from the latest surface data time—for example, 1800 UTC.

cating that they learned some basic patterns. That level of learning is probably to be expected given the limited kind, amount, and spacing of the data input.

4. Neural network analysis

In statistical forecast methods, and even in expert-system forecasts, it is not difficult to understand how a given input is transformed into a forecast. Unfortunately, neural networks are complex structures. The networks developed in this experiment have nearly 5000 connections apiece. Thus, large neural networks such as the ones developed here are "black boxes" when it comes to discerning how input becomes output. Nevertheless, there are some approaches that can help in this regard.

a. Sensitivity tests

One approach is to test the neural networks with simple input and look at their responses. If the responses are not reasonable, then the networks probably cannot be trusted to give dependable output on more complex input.

For the first test, the lifted index values vary from their highest (+5) to their lowest (−12) acceptable values at every point in the domain while holding all moisture divergence values to zero. Intuitively, the lower the LI values are, the more unstable the low-level air mass is, so the higher the likelihood of thunderstorms. Figure 6 shows that both networks' output increases with a lower lifted index, as hoped. Interestingly, NN0 appears to be less sensitive to changes in LI throughout the entire range than NN1. NN0 is most sensitive in the LI range from −1 to −7, while NN1's sensitivity is the most acute when LI values are lower than −5.

Similarly, in a second test, moisture divergence varies from +30 to −60 at all points while holding all LI values to zero. Again, the lower the moisture divergence is, the more low-level forcing exists; therefore, the chances for thunderstorms are higher. Figure 7 confirms intuition since a decrease in moisture-divergence input increases both networks' output, obviously much more with NN1 than with NN0.

Hirt (1982) and others have shown that thunderstorms are more likely to develop to the east of a convergence maximum. To see how the neural networks respond to that kind of input, a 3 × 3 subgrid of minimum divergence (−60) was placed at various locations within the larger grid and all other points were set to zero (Fig. 8). As seen in Fig. 9, the neural networks do maximize when convergence is to the west of the point of interest. A 3 × 3 subgrid of maximum diver-

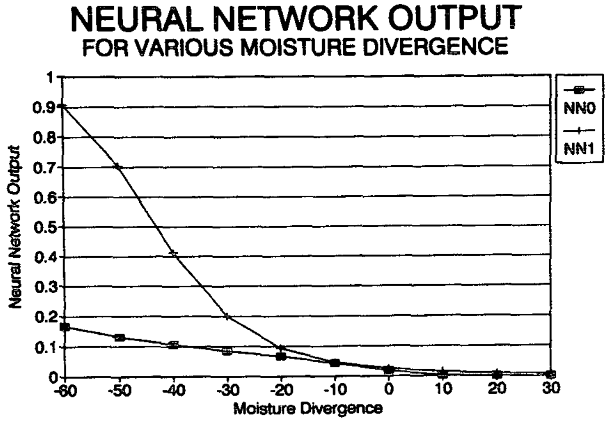

FIG. 7. Same as Fig. 6 except for neural-network output for various moisture divergence values.

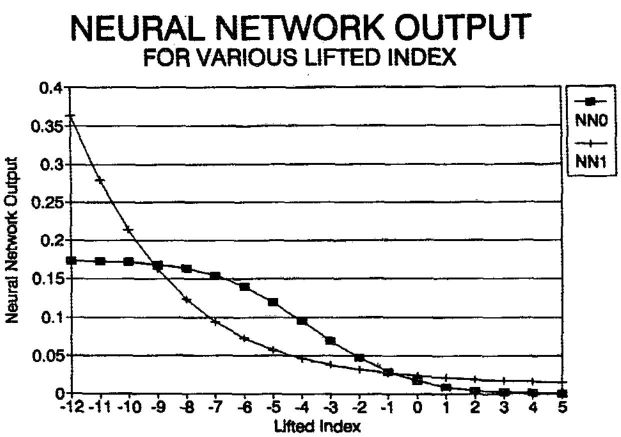

FIG. 6. Neural-network output for various lifted-index values. Output is a dimensionless number between zero (no significant thunderstorms forecast) and one (significant thunderstorms forecast).

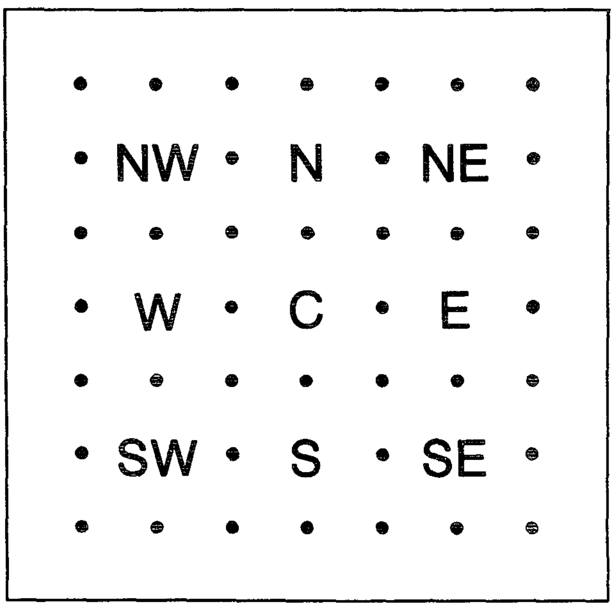

FIG. 8. Diagram showing various 3 × 3 subgrid locations within the 7 × 7 grid. Location labels are directions from the center, C.

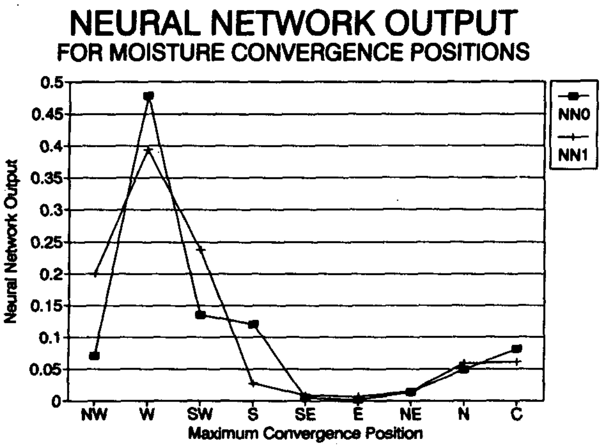

FIG. 9. Same as Fig. 6 except for neural-network output for various moisture-convergence maximum positions.

gence (30) was similarly positioned in the larger grid to observe the effects of moisture divergence on the networks. The outcome was almost opposite to the maximum network output when divergence is to the east or southeast (Fig. 10). Note that the effect of a divergence center on network output is an order of magnitude less than that of a convergence center.

Hirt noted that a convergence–divergence couplet is even more favorable for thunderstorm development between the centers than the condition where just convergence is to the west. All combinations of convergence–divergence couplets were tested in the networks, and the best convergence–divergence associations were a west–east couplet for NN0 (output = 0.829) and a west–southeast couplet for NN1 (output = 0.618). These results illustrate the nonlinear nature of neural networks and their ability to recognize important patterns. While divergence to the east of the point of interest is not too important to thunderstorm development by itself, adding some to the east of a convergence maximum nearly doubles the significance of convergence to the west (compare with Fig. 9.)

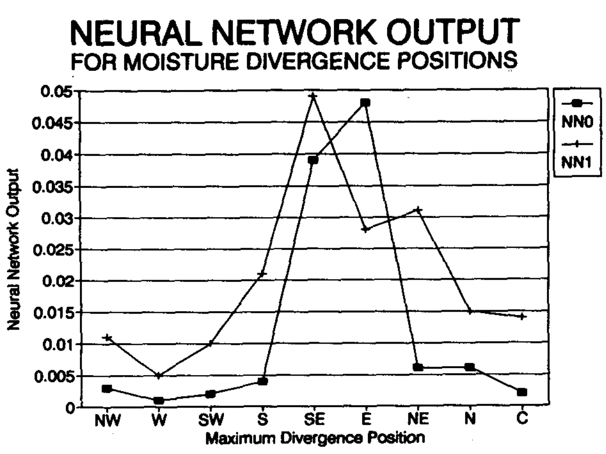

FIG. 10. Same as Fig. 6 except for neural-network output for various moisture-divergence maximum positions.

Old thunderstorm outflow boundaries can also influence new thunderstorm formation and many times are seen on surface charts by strong instability gradients north of east–west boundaries (Hales and Doswell 1982). The neural networks were tested for their proficiency in identifying this pattern similar to the testing for convergence–divergence patterns. Various LI fields were divided in half with maximum LI (+5) in one half of the domain and minimum LI (−12) in the other. Moisture divergence was set to zero everywhere. To summarize the results, both networks preferred the east–west boundary alignment with NN0 output at a very high 0.914 and NN1 output at 0.720. Both networks liked slight variations of this orientation nearly as well.

b. Hidden neuron analysis

A more direct technique to reveal neural-network "thinking" is to look at the individual connection weights between the hidden neurons and the output. The hidden neurons with the highest absolute-value weight connections have the most influence on the

NEURAL NETWORK #0
Hidden Neuron #36 weight = -3.558

Lifted Index

-.033	+.084	-.186	+.185	+.232	-.162	-.161
+.074	+.194	-.048	+.100	-.205	-.164	-.027
-.203	+.044	-.133	-.106	+.024	+.136	+.123
-.090	+.221	-.072	+.010	+.019	-.102	-.203
-.062	+.067	-.058	-.223	-.100	-.112	-.112
-.189	+.168	-.121	+.061	-.177	+.102	-.129
+.240	-.037	-.215	-.151	-.187	-.024	-.004

Moisture Divergence

+.044	-.246	+.145	+.186	-.037	+.040	-.001
+.118	+.239	-.223	+.017	-.176	-.192	-.079
-.030	-.061	-.052	+.073	-.209	-.044	-.049
-.008	-.023	-.184	+.148	+.161	+.171	+.029
+.144	-.097	-.093	+.221	+.049	-.220	+.106
+.089	+.066	-.122	+.062	-.132	-.035	+.101
+.127	-.244	-.237	-.065	-.037	+.135	-.070

FIG. 11. Connection weights for hidden neuron #36, NN0. Within the dashed lines are continuous areas of large weights with the same sign.

output. In turn, one can examine the input-connection weights of those special hidden neurons to see how the input affects them.

Figures 11 and 12 show this analysis for the highest weighted hidden neuron for each network. In the first example (Fig. 11), recall that in NN0, low values of LI (unstable air) and low moisture divergence (moisture convergence) are positive influences on network output. Since the output connection weight for neuron #36, NN0, is negative (−3.558), a negative summation of input connections will produce the largest output. The most negative input-connection weights will produce the most negative summation if positively stimulated. As illustrated in the figure, most of the negative weights in the LI portion are to the south and southeast of the forecast point. Therefore, when unstable air is located to the south and southeast, network output can be high. In the moisture-divergence portion, there are negative weights to the northeast, immediate west, and south-southwest. There are positive weights near the center and to the immediate east. Moisture convergence where the weights are negative and divergence where the weights are positive will help produce the negative summation desired for high positive output. This resembles a frontal wave pattern with the wave just to the west of the point of interest. Unstable air would be located to the south and southeast of the wave. Therefore, only this one hidden neuron knows one of the most favorable patterns for thunderstorm development known to forecasters.

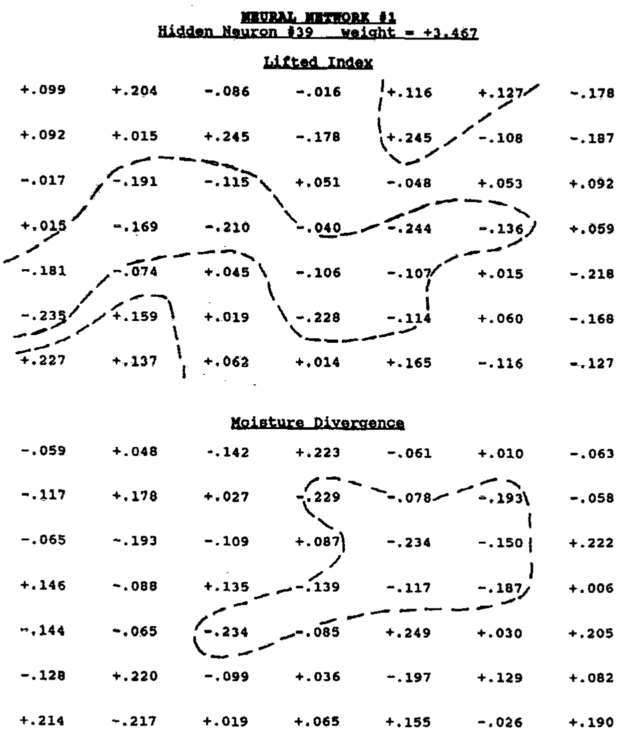

FIG. 12. Same as Fig. 11 but for hidden neuron #39, NN1.

A similar look at hidden neuron #39, NN1, (Fig. 12) reveals a different pattern that is not quite as easy to see. The output-connection weight here is positive, but then the influence of high instability and high moisture convergence are opposite from NN0. So where there are negative input-connection weights and low LI and moisture-divergence values (favorable thunderstorm conditions), hidden-neuron output is high, which is similar to the previous example. So does this hidden neuron represent a pattern with an east–west axis of instability and stable air to the far southwest and north-northeast, a dry line, and a thunderstorm outflow boundary pattern? The associated favorable moisture divergence pattern would support this assumption.

As one has probably surmised by now, a direct analysis of all the hidden neurons would be difficult. Many of the hidden neurons probably even group together to "know" a particular favorable pattern for thunderstorm development, so it is practically impossible to understand the "black box." The conclusions of this analysis are not very satisfying to scientists. Acceptance comes from how well the networks have learned real patterns.

5. Neural network significant thunderstorm forecast

If the neural network forecasts can accurately forecast significant thunderstorm areas, then they will have real value to meteorologists. Three days were randomly chosen from the database, and network output for all the grid points was calculated and mapped. Both neural networks showed substantial skill when compared subjectively with actual significant thunderstorm occurrence. Combining both forecasts by averaging the two outputs at each grid point produced even better results by reducing the areas positively forecast by each network individually to the area where both networks overlapped (agreed). The three cases are shown in Fig. 13.

The output varies from zero to one and looks like an areal probability forecast, but it is not a true probability in a statistical sense. Based on these cases, as well as daily fields from late spring 1991, it appears that large areas of 0.3 or greater are areas with good potential, and areas with a maximum greater than 0.7 are almost certain to have significant convection. It also appears that neural-network output not only shows where the highest "probability" of significant convection is located but also that the most significant storm systems, that is, the largest and most severe, (not shown specifically in Fig. 13) occur in the areas of highest output.

The combined neural-network outlook (NNET) for the continental United States and adjacent areas has been available to NSSFC forecasters hourly since mid-April 1991 on the center's VDUC computer system. Both LI and moisture convergence are computed dif-

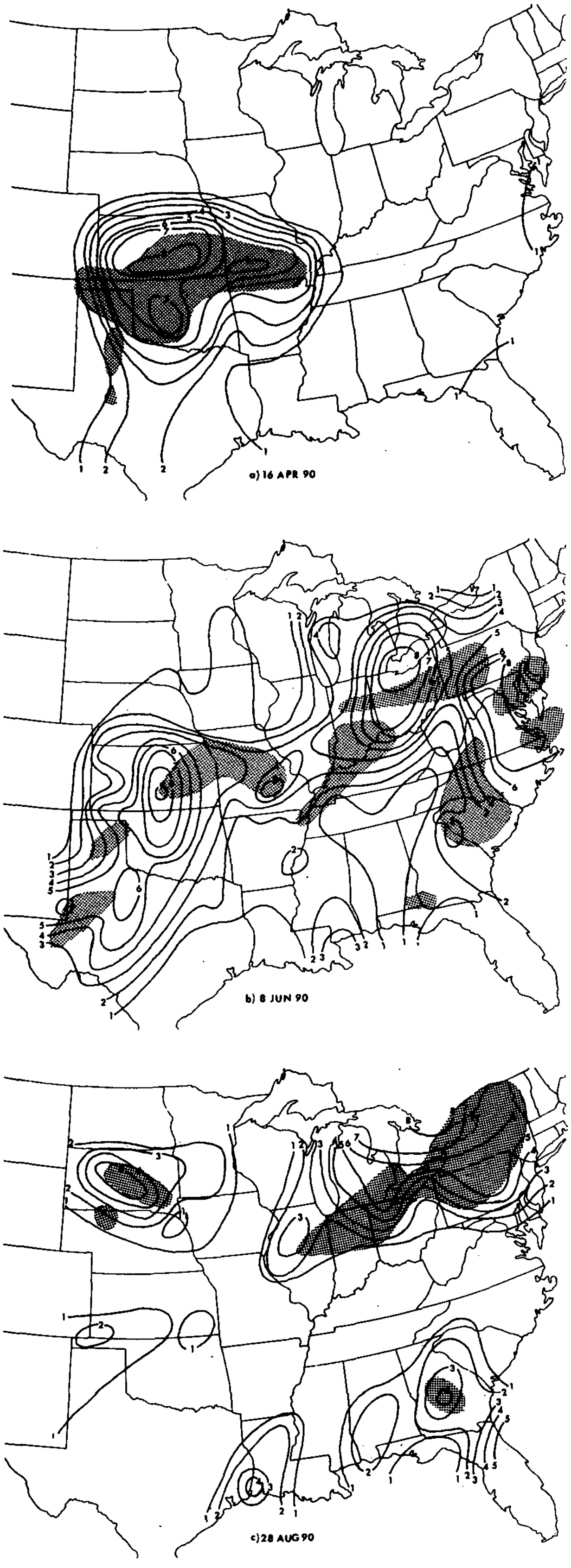

FIG. 13. NNET output on 1800 UTC for three days: (a) 16 April 1990, (b) 8 June 1990, and (c) 28 August 1990. Contours are NNET output/10 and stippled areas are the areas of significant thunderstorms subsequently needing WST issuances from 2100 to 0100 UTC.

ferently than those on CSIS. On the VDUC system, the LI fields are now calculated with numerical-model 500-mb forecast temperatures. The new lifted-index fields are similar but better reflect changes in the 500-mb temperatures. Moisture-flux convergence is now calculated instead of moisture divergence. Moisture-flux convergence is only slightly different from moisture divergence (other than the sign) in that the former adds moisture advection to the moisture convergence. Since moisture convergence is the dominant term in the moisture-flux convergence equation, there is usually not much difference between the patterns most of the time (Bothwell 1988). However, Bothwell noted that sometimes the advection term can be significant. The more substantial difference between CSIS fields and VDUC fields is that the latter are calculated on one-half-degree grids, while the former are figured on one-degree grids. The grid-size–dependent nature of derivative computations yields more detailed fields with the VDUC system than with the CSIS system. The NNET fields appear to be only slightly affected.

Although NNET was developed from 1800 UTC data, computing it at other times of the day has produced forecast fields of similar usefulness. It is quite interesting to see hour-by-hour changes of NNET output as it forecasts the usual diurnal trend of convection. Areas of maximum output increase in size and magnitude from early morning to late afternoon; then they decrease into the night.

NNET has difficulty predicting thunderstorms that are forced by processes not seen in the surface data. These include overrunning thunderstorms and those associated with some positive vorticity centers aloft. Additionally, NNET does not do well in areas where there is no surface data or where the surface data is not representative. These areas include coastal areas of the United States and mountainous areas from the Rockies westward.

6. Impact of neural network forecasts

The author's personal experience from using NNET on a daily basis is that by making adjustments to NNET output based on current convective trends, the size of his WST outlooks were substantially reduced (compared with those made with older techniques in previous years) without an adverse affect on the ability to capture WST issuances in the outlooks. This was tested by verifying some of his WST outlooks for June and July 1990 and 1991 before and after NNET. Outlooks verified were east of the Rocky Mountains at issuance times of 1855, 0055, and 0955 UTC. Each of these outlook times poses a different forecast problem. The

1855 UTC outlook challenge is to forecast the major late-afternoon convection. The 0055 UTC outlook question pertains to the length significant thunderstorms will continue. The 0955 UTC outlook may be the most difficult of the three times because it is a forecast for strong convection at the daily climatological thunderstorm minimum. Each 2-month period in both years was about equally active convectively as measured by the number of subsequent WSTs issued.

Each outlook during the period was verified by seeing how well subsequent WST issuances were captured in the outlook. For example, the four WST hourly issuances at 2155 UTC through 0055 UTC verified an 1855 UTC outlook. The union of the outlook area and the area of ensuing WSTs divided by the total WST issuance area defined a probability of detection (POD). The outlook area not capturing WSTs divided by the total outlook area defined a false-alarm ratio (FAR) (Charba and Klein 1980). A critical success index (CSI) can be calculated using a standard formula, CSI $= (\mathrm{POD}^{-1} + (1 - \mathrm{FAR})^{-1} - 1)^{-1}$.

Table 1 gives the verification results. Indeed, the median outlook area size for 1991 was 36% smaller than the median size for 1990, and the total area outlooked per issuance (more than one outlook area could be issued at one issuance time) was 29% smaller for the same comparison. The POD for 1991 is slightly higher than the POD for 1990 and, combined with the reduced 1991 FAR, results in a large improvement in the CSI results. Note that NNET had only been operational for a little more than one month in June 1991, so WST outlooks are likely to continue improving as the author and other meteorologists climb higher up the learning curve on how to use NNET in their forecasts.

One qualitative observation of the potential impact of NNET on WST outlooks is that NNET seems to have the ability to highlight where the strongest and the most intense thunderstorms will be located. Areas of high NNET output generally have larger storms in them and have more solid coverage of significant thunderstorms. Additionally, in some cases NNET has been able to forecast late-night or early-morning activity that would not have been forecast normally given the time of day.

TABLE 1. Verification results for WST outlooks for June/July 1990 and 1991.

	Median area	Total area per forecast	FAR	POD	CSI	Total WSTs issued
1990						
1855	97056	277608	.760	.493	.192	120
0055	82391	139667	.793	.527	.175	82
0955	37916	25266	.743	.189	.121	79
All	80671	127499	.772	.441	.177	281
1991						
1855	64521	212998	.722	.403	.197	145
0055	38809	106910	.647	.596	.285	86
0955	0	0	—	.000	—	45
All	51870	90272	.688	.459	.228	276

Note: All times are UTC. All areas are in square nautical miles.

Other forecasters have found NNET helpful. The forecasters in the FA/Inflight Advisory section of NAWAU occasionally work in the Convective SIGMET Unit in order to maintain proficiency and to occasionally fill in. They do not have the experience of the regulars and by their own admission sometimes feel less confident about their outlooks as compared with those of the regulars. They also have found that they can favorably reduce the size of their outlooks with NNET. Feedback from those infrequent workers who have tried NNET has been very positive.

Additionally, at least one NSSFC lead forecaster has used NNET output in severe weather watch formulation. NNET's design is primarily for significant, WST-type thunderstorms, not necessarily severe. However, the union of these two sets of thunderstorms is large. The time frame for NNET is also about the same as those for watches. Since NNET forecasts 2–3 h beyond the present, it says nothing about the immediate prospects of a thunderstorm system but says much about its prospects late in a valid watch period. NNET should add value to the severe weather watch program even though it was not created specifically for that problem.

NNET is succeeding in both the goals of AI techniques mentioned in section 2. NNET has boosted the author up the "significant thunderstorm forecast" learning curve by doing preliminary pattern recognition and eliminating areas of improbable development. That has allowed more time to concentrate on the favorable areas and to refine them further. NNET also has aided less experienced forecasters who work infrequently as WST meteorologists. Even if they do not understand why a particular pattern is favorable for forecasting significant thunderstorms in one area and not in another, they issue better forecasts when they incorporate NNET in their routine. By getting guidance to where favorable and unfavorable conditions are located, they can begin to understand the dynamical processes of thunderstorm development and eventually have more confidence in their forecasts.

7. Conclusions

It is important to note that NNET and other potential neural networks are nothing more than pattern-recognition diagnostic techniques with some short-term predictive skill. NNET was not designed to automate WST outlooks, nor should any AI technique be designed to replace meteorologists.

Nevertheless, in the future, artificial intelligence can help meteorologists sort through the expansion of meteorological information and help relieve the probable data overload that such an expansion will bring. NNET is an initial step that demonstrates how neural networks can systematize pattern recognition and help solve important meteorological problems. A neural network's ability to recognize patterns will probably be useful in radar and satellite analysis when greater computer power becomes more available. Neural networks could enhance numerical-model output and analysis and perhaps give new insights into old forecasting problems.

Acknowledgments. Many thanks go to Phillip Bothwell, Jack Hales, Doug Mathews, Peter Browning, and Joseph Schaefer for their helpful reviews. Additional thanks go to Phil and to Peter for getting me up to speed on VDUC programming so NNET could become a reality.

REFERENCES

Bothwell, P. D., 1988: Forecasting convection with the AFOS data analysis programs (ADAP-version 2.0). NOAA Tech. Memo. NWS SR-122, 91 pp. [Available from Scientific Services Division, Southern Region, Fort Worth, TX.]

Bullas, J. M., J. C. McLeod, and B. de Lorenzis, 1990: Knowledge augmented severe storms predictor (KASSPr)—An operational test. *Proc. 16th Conf. on Severe Local Storms,* Kananaskis Park, Alta., Canada, Amer. Meteor. Soc., 106–111.

Caudill, M., 1990: *Neural Networks Primer.* Miller Freeman Publications, 64 pp.

——, 1991: Neural network training tips and techniques. *AI Expert,* **6**(1), 56–61.

Charba, J. P., 1979: The 2–6-h severe local storm probabilities: An operational forecasting system. *Mon. Wea. Rev.,* **107,** 268–282.

——, and W. H. Klein, 1980: Skill in precipitation forecasting in the National Weather Service. *Bull. Amer. Meteor. Soc.,* **61,** 1546–1555.

Darkow, G. L., and R. L. Livingston, 1975: Hourly surface static energy analysis as a delineator of thunderstorm outflow areas. *Mon. Wea. Rev.,* **103,** 817–822.

Doswell, C. A., III, 1982: The operational meteorology of convective weather. Volume I: Operational mesoanalysis. NOAA Tech. Memo. NWS NSSFC-5. [Available from National Severe Storms Forecast Center, Kansas City, MO.]

Edman, D. A., 1989: A comparison of the surface based hourly lifted indices produced by the NSSFC CSIS and AFOS ADAP algorithms. *Proc. 12th Conf. on Weather Analysis and Forecasting,* Monterey, CA, Amer. Meteor. Soc., 93–96.

Frankel, D., I. Schiller, J. S. Draper, and A. A. Barnes, 1990: Investigation of the prediction of lightning strikes using neural networks. *Proc. 16th Conf. on Severe Local Storms,* Kananaskis Park, Alta., Canada, Amer. Meteor. Soc., 7–12.

Hales, J. E., Jr., and C. A. Doswell III, 1982: High resolution diagnosis of instability using hourly surface lifted parcel temperatures. *Proc. 12th Conf. on Severe Local Storms,* San Antonio, TX, Amer. Meteor. Soc., 172–175.

Hirt, W. D., 1982: Short-term prediction of convective development using dew point convergence. *Proc. 9th Conf. on Weather Analysis and Forecasting,* Seattle, WA, Amer. Meteor. Soc., 201–205.

Livingston, R. L., and L. F. Wilson, 1986: Relating antecedent surface conditions to violent tornado-producing thunderstorms. *Proc. 11th Conf. on Weather Analysis and Forecasting,* Kansas City, MO, Amer. Meteor. Soc., 229–234.

Maddox, R. A., and C. A. Doswell III, 1982: Forecasting severe thunderstorms: A brief evaluation of accepted techniques. *Proc. 12th Conf. on Severe Local Storms,* San Antonio, TX, Amer. Meteor. Soc., 92–95.

McCann, D. W., 1988: LIVV—A two chart medium-range severe thunderstorm forecast. *Proc. 15th Conf. on Severe Local Storms,* Baltimore, MD, Amer. Meteor. Soc., 476–479.

McNulty, R. P., 1981: A statistical approach to short-term thunderstorm outlooks. *J. Appl. Meteor.,* **20,** 765–771.

Moninger, W. R., 1990: The artificial intelligence shootout: A comparison of severe storm forecasting systems. *Proc. 16th Conf. on Severe Local Storms,* Kananaskis Park, Alta., Canada, Amer. Meteor. Soc., 1–6.

Ostby, F. P., Jr., 1975: An application of severe storm forecast techniques to the outbreak of June 8, 1974. *Proc. 9th Conf. on Severe Local Storms,* Norman, OK, Amer. Meteor. Soc., 7–12.

——, 1984: Use of CSIS in severe weather prediction. *SPIE Vol. 481—Recent Advances in Civil Space Remote Sensing,* Soc. of Photo-Optical Instrumentation Engineers, 78–83.

Stanley, J., 1988: *Introduction of Neural Networks.* California Scientific Software, 255 pp.

Waldstreicher, J. S., 1989: A guide to utilizing moisture flux convergence as a predictor of convection. *Natl. Wea. Dig.,* **14**(4), 20–35.

Weaver, J. F., and R. S. Phillips, 1990: An expert system application for forecasting severe downslope winds at Ft. Collins, Colorado, U.S.A. *Proc. 16th Conf. on Severe Local Storms,* Kananaskis Park, Alta., Canada, Amer. Meteor. Soc., 13–15.